

## PDF hosted at the Radboud Repository of the Radboud University Nijmegen

The following full text is a publisher's version.

For additional information about this publication click this link.

<http://hdl.handle.net/2066/91660>

Please be advised that this information was generated on 2017-12-06 and may be subject to change.

## Contactless electroreflectance of AlGaIn/GaN heterostructures deposited on *c*-, *a*-, *m*-, and (20.1)-plane GaN bulk substrates grown by ammonothermal method

R. Kudrawiec,<sup>1,a)</sup> M. Rudziński,<sup>2</sup> M. Gladysiewicz,<sup>1</sup> L. Janicki,<sup>1</sup> P. R. Hageman,<sup>3</sup> W. Strupiński,<sup>2</sup> J. Misiewicz,<sup>1</sup> R. Kucharski,<sup>4</sup> M. Zając,<sup>4</sup> R. Doradziński,<sup>4</sup> and R. Dwiliński<sup>4</sup>

<sup>1</sup>*Institute of Physics, Wrocław University of Technology, Wybrzeże Wyspiańskiego 27, 50-370 Wrocław, Poland*

<sup>2</sup>*Institute of Electronic Materials Technology, Wólczyńska 133, 01-919 Warsaw, Poland*

<sup>3</sup>*Institute for Molecules and Materials, Radboud University, Heyendaalseweg 135, 6525AJ Nijmegen, The Netherlands*

<sup>4</sup>*AMMONO sp. z.o.o., Czerwonego Krzyża 2/31, 00-377 Warsaw, Poland*

(Received 10 November 2010; accepted 27 January 2011; published online 23 March 2011)

Room temperature contactless electroreflectance (CER) has been applied to study optical transitions and the distribution of the built-in electric field in AlGaIn/GaN heterostructures grown on *c*-, *a*-, *m*-, and (20.1)-plane GaN substrates obtained by the ammonothermal method. It has been clearly shown that polarization effects in the AlGaIn/GaN heterostructures grown on the *c*-plane lead to a strong built-in electric field in the AlGaIn layer. The aforementioned field was determined to be  $\sim 0.43$  MV/cm from the period of Franz–Keldysh oscillations (FKOs). In addition, polarization effects lead to the formation of a two dimensional electron gas at the AlGaIn/GaN interface, which screens the band bending modulation in the GaN buffer layer, and, therefore, GaN-related excitonic transitions are not observed for this heterostructure. Such features/effects are also not observed in the AlGaIn/GaN heterostructures grown on nonpolar and semipolar GaN substrates because any strong polarization effects are not expected in this case. For these heterostructures, very strong and sharp GaN excitonic resonances are clearly visible in CER spectra. The resonances are very similar to the excitonic transitions observed for the GaN epilayers deposited on nonpolar and semipolar substrates. Moreover, there is a very weak AlGaIn-resonance without FKO for nonpolar and semipolar heterostructures instead of the strong AlGaIn-related FKO, which is typical of polar AlGaIn/GaN heterostructures. © 2011 American Institute of Physics. [doi:10.1063/1.3560537]

### I. INTRODUCTION

Due to strong spontaneous and piezoelectric polarization in III-N<sup>1,2</sup> a triangular quantum well is formed at the AlGaIn/GaN interface when the heterostructure is grown along the polar direction (*+c*). Electrons accumulate at this interface forming a two dimensional electron gas (2DEG), which reaches a concentration of  $\sim 10^{13}$  cm<sup>-2</sup>, even without any intentional doping in the system.<sup>2</sup> Currently, this phenomenon is widely exploited in the field-effect transistor (FET) heterostructures operating with high powers at high temperatures.<sup>3</sup> However, this solution has some limitations because a large carrier density in the 2DEG is present even at the depletion mode. Some of these limitations can be overcome in the AlGaIn/GaN heterostructures grown along nonpolar directions,<sup>4-7</sup> but this approach was not intensively explored because of the deficient access to native nonpolar GaN substrates. The recent progress in the ammonothermal growth of GaN crystals allows the fabrication of GaN substrates with various crystallographic orientations including polar and nonpolar as well as semipolar orientations.<sup>8-11</sup> It opens the possibility of the growth of

AlGaIn/GaN heterostructures along various crystallographic orientations in GaN. However, so far such studies were not intensively conducted, and a lot of fundamental properties are still unexplored for such heterostructures. One of them is the distribution of the built-in electric field in AlGaIn/GaN heterostructures that is responsible for the formation of 2DEG at the AlGaIn/GaN interface. In this paper, we applied contactless electroreflectance (CER) spectroscopy to study optical transitions and the built-in electric field in the AlGaIn/GaN heterostructures grown by metalorganic chemical vapor deposition (MOCVD) on *c*-, *a*-, *m*-, and (20.1)-plane GaN substrates obtained by the ammonothermal method.

CER spectroscopy is a very powerful absorptionlike technique to study optical transitions in various semiconductor structures, including quantum dots,<sup>12</sup> quantum wells,<sup>13</sup> and FETs.<sup>14-19</sup> Its derivative character allows both the elimination of the background signal and detection of very weak optical transitions even at room temperature. Due to the Franz–Keldysh effect,<sup>20</sup> this method can be applied to investigate the built-in electric field in AlGaIn/GaN transistor heterostructures<sup>16-19</sup> as well as the type of band bending.<sup>19,21</sup> CER spectroscopy has been applied many times to study optical transitions and the built-in electric field in polar AlGaIn/GaN heterostructures.<sup>16-19</sup> It has been shown that

<sup>a)</sup>Author to whom correspondence should be addressed. Electronic mail: robert.kudrawiec@pwr.wroc.pl.

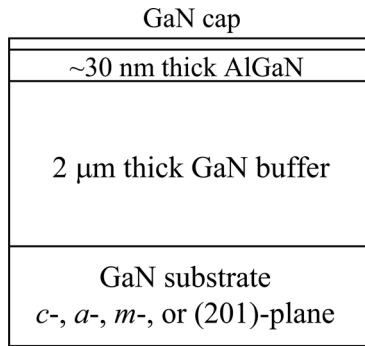


FIG. 1. Layer sequence in AlGaIn/GaN heterostructures grown on bulk GaN substrates of various crystallographic orientations.

this technique enables detecting the formation of 2DEG at the AlGaIn/GaN interface in a contactless manner<sup>22</sup> as well as determining the built-in electric field in the AlGaIn barrier<sup>16–19</sup> and its changes upon SiN deposition.<sup>17</sup> Therefore, it is expected that CER spectroscopy will provide similar information for the AlGaIn/GaN heterostructures grown on nonpolar and semipolar GaN substrates.

## II. EXPERIMENTAL DETAILS

AlGaIn/GaN heterostructures (see the layer sequence in Fig. 1) were grown by MOCVD (with a RF heated AIXTRON AIX-200 low pressure horizontal reactor) simultaneously on *c*-, *a*-, *m*-, and (20.1)-plane GaN substrates obtained by the ammonothermal method. Trimethylgallium, trimethylaluminum, and ammonia were used as precursors and H<sub>2</sub> as the carrier gas. For comparison purposes, a set of 2 μm thick GaN layers were grown under the same conditions. CER measurements were performed at room temperature in a capacitor with the top electrode made from a copper-wire mesh, which was semitransparent for light. This electrode was kept at a distance of ~0.5 mm from the sample surface, while the sample itself was fixed on the bottom copper electrode. A maximum peak-to-peak alternating voltage of ~3.0 kV with the frequency of 285 Hz was applied. Other relevant details of CER measurements are described in Ref. 19.

## III. RESULTS AND DISCUSSION

Figures 2(a)–2(d) show the CER spectra of the AlGaIn/GaN heterostructure and GaN layer grown on the *c*-, *a*-, *m*-, and (20.1)-plane GaN substrate, respectively. To enable comparison between the above-mentioned CER spectra, the same scale and spectral range are used. The CER features related to GaN and AlGaIn layers are observed for all heterostructures, but their shape and intensity strongly depend on the crystallographic orientation.

For the heterostructure grown on *c*-plane GaN [Fig. 2(a)], the spectrum is very similar to the CER spectra previously reported for AlGaIn/GaN heterostructures, see Refs. 16–19, 21, and 22. The observed AlGaIn signal possesses a characteristic Franz–Keldysh oscillation (FKO), the period of which depends on the built-in electric field in the AlGaIn layer. A conventional method to determine the built-in electric field from FKO is to use an asymptotic expression for electro-reflectance<sup>20</sup>

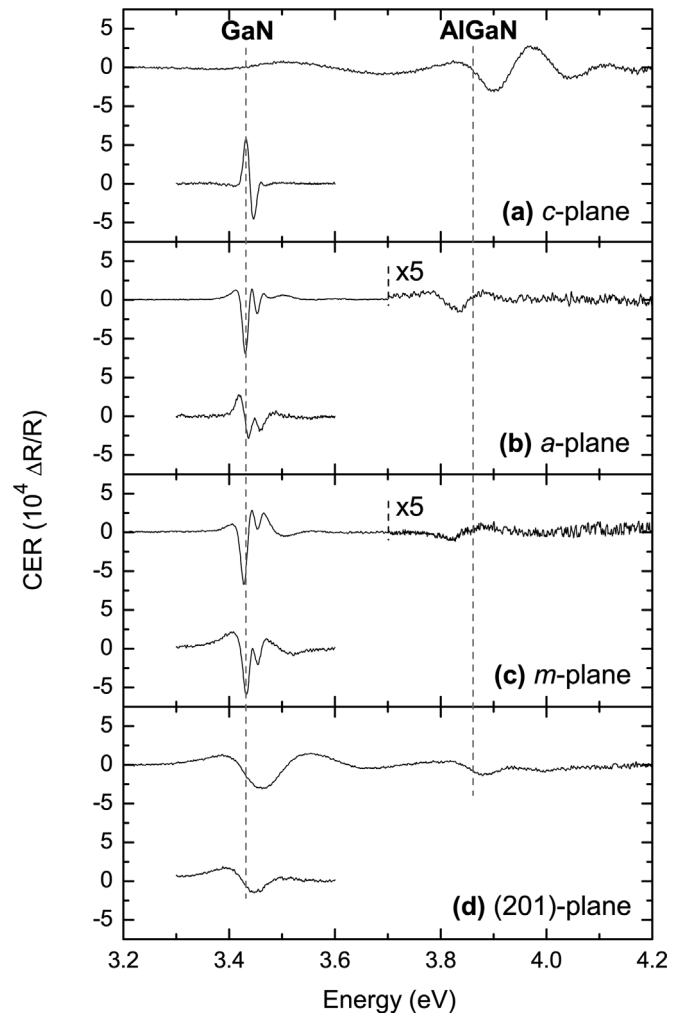


FIG. 2. Room temperature contactless electroreflectance spectra measured for AlGaIn/GaN heterostructures (top spectra) and 2 μm thick GaN layers (bottom spectra) grown on (a) *c*-, (b) *a*-, (c) *m*-, and (d) (20.1)-plane bulk GaN substrates.

$$\frac{\Delta R}{R} \propto \exp\left[\frac{-2\Gamma\sqrt{E-E_g}}{(\hbar\theta)^{3/2}}\right] \cdot \cos\left[\frac{4}{3}\left(\frac{E-E_g}{\hbar\theta}\right)^{3/2} + \phi\right] \times \frac{1}{E^2(E-E_g)}, \quad (1)$$

$$(\hbar\theta)^3 = \frac{e^2\hbar^2 F^2}{2\mu},$$

where  $\hbar\theta$  is the electro-optic energy,  $\Gamma$  is the line width,  $\phi$  is an angle,  $F$  is the electric field, and  $\mu$  is the electron-hole reduced mass (for AlGaIn  $\mu$  is assumed to be 0.2  $m_0$  after Ref. 23). The extrema of FKO are given by

$$n\pi = \phi + \frac{4}{3}\left[\frac{(E_n - E_g)}{\hbar\theta}\right]^{3/2}, \quad (2)$$

where  $n$  is the index of the  $n$ th extremum and  $E_n$  is the corresponding energy. A plot of  $(E_n - E_g)^{3/2}$  versus  $n$  yields a straight line with a slope proportional to  $F$ . An analysis of the AlGaIn-related FKO period for the AlGaIn/GaN heterostructure grown on the *c*-plane GaN substrate is shown in Fig. 3. The built-in electric field in the AlGaIn layer has been determined from this plot to be ~0.43 MV/cm.

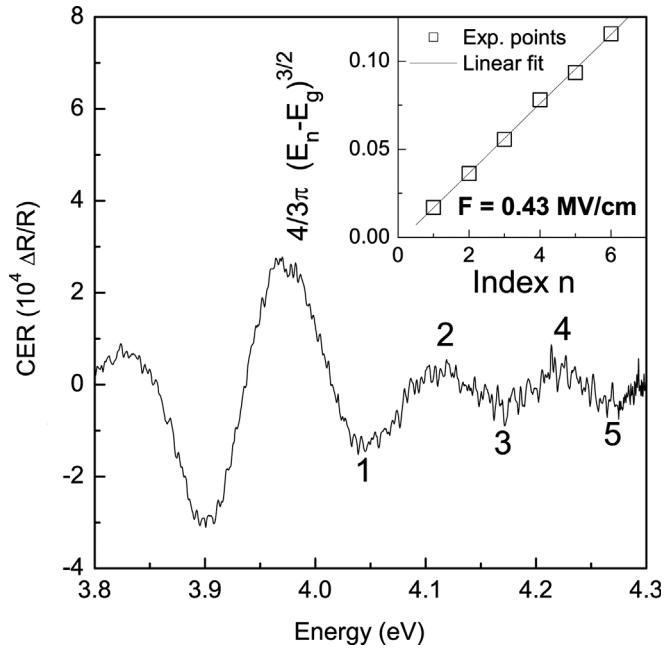


FIG. 3. Room temperature contactless electroreflectance spectrum of AlGaIn/GaN heterostructure grown on *c*-plane GaN substrate in the vicinity of AlGaIn transition together with the analysis of the period of Franz-Keldysh oscillation (inset).

For the AlGaIn/GaN heterostructures grown on nonpolar GaN substrates, any AlGaIn-related FKO's are not observed in CER spectra. In this case, the shape of CER resonance is typical of an excitonic or band-to-band absorption in a layer with a weak built-in electric field. For such an absorption, the line shape of CER resonance is described by Aspnes formula<sup>24</sup>

$$\frac{\Delta R}{R}(E) = \text{Re}[C \cdot e^{i\vartheta} (E - E_0 + i \cdot \Gamma)^{-m}], \quad (3)$$

where  $E_0$  and  $\Gamma$  are the energy and the broadening parameter of the transition, and  $C$  and  $\vartheta$  are the amplitude and phase of the resonance, respectively. The term  $m$  refers to the type of optical transitions and equals 2 for an excitonic and 2.5 for a band-to-band transition. Figures 4(a)–4(c) show the analysis of the AlGaIn-related transition for heterostructures grown on *a*-, *m*-, and (20.1)-plane GaN substrates together with the fitting curves (thick gray lines) and the moduli of CER resonances (dashed lines), which are calculated from Eq. (4)

$$\Delta\rho(E) = \frac{|C|}{[(E - E_0)^2 + \Gamma^2]^{m/2}} \quad (4)$$

with parameters taken from the fit. It has been observed that the energy gap of the AlGaIn layer grown simultaneously in the same process on GaN substrates with various crystallographic orientations is different. It means that the aluminum incorporation into the AlGaIn alloy depends on the growth direction. This conclusion has been confirmed by x-ray diffraction measurements, and it will be discussed in detail elsewhere.

As seen in Fig. 2(a), GaN excitonic transitions are not observed for the polar AlGaIn/GaN heterostructure, whereas

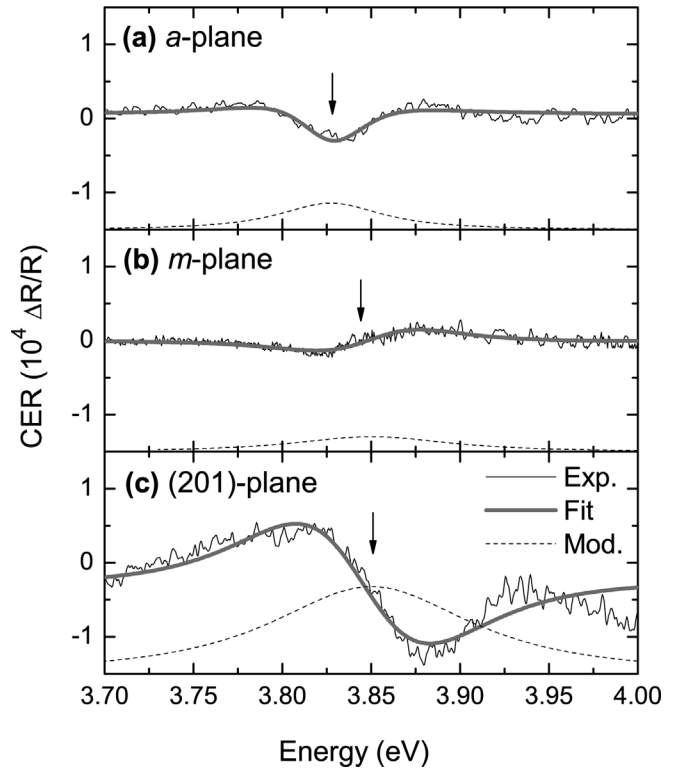


FIG. 4. Room temperature contactless electroreflectance spectra of AlGaIn/GaN heterostructures grown on (a) *a*-, (b) *m*-, and (c) (20.1)-plane GaN substrate in the vicinity of AlGaIn transition together with the fit (thick gray lines) by Eq. (3) and the moduli of CER resonances (dashed lines).

in the case of the GaN epilayer grown on the *c*-plane GaN as well as AlGaIn/GaN heterostructures and GaN layers grown on nonpolar substrates they are clearly visible, see Fig. 2. This phenomenon is associated with the screening of band bending modulation in the GaN buffer layer by 2DEG.<sup>16,22</sup> Figure 5(a) schematically shows band bending and its modulation in the AlGaIn/GaN heterostructure grown on the *c*-plane GaN. In addition, the possible optical transitions in each part of this structure are marked by arrows in this scheme, and their character is described in the figure caption. According to this sketch, excitonic transitions are expected far from the AlGaIn/GaN interface where the band bending is weak, see the transition labeled as (iv) in Fig. 5(a). However, no band bending modulation is expected in this region because of the screening of electromodulation in this layer. It explains why excitonic transitions are not observed for this heterostructure. The weak and broad CER feature at  $\sim 3.5 - 3.6$  eV [see Fig. 2(a)] is attributed to light absorption in the GaN cap layer (that is, it is an optical transition in the GaN surface quantum well<sup>25</sup>) and/or band-to-band absorption in the GaN buffer layer near the AlGaIn/GaN interface, see (iii) arrows in Fig. 5(a).

The strong excitonic transitions in the AlGaIn/GaN heterostructures grown on nonpolar substrates [see Figs. 2(b) and 2(c)] mean that the band bending in the GaN buffer layer is not strong because such sharp excitonic transitions are expected for layers with a weak band bending. In addition, it means that the band bending in the GaN buffer layer is effectively modulated in these samples (that is, no screening

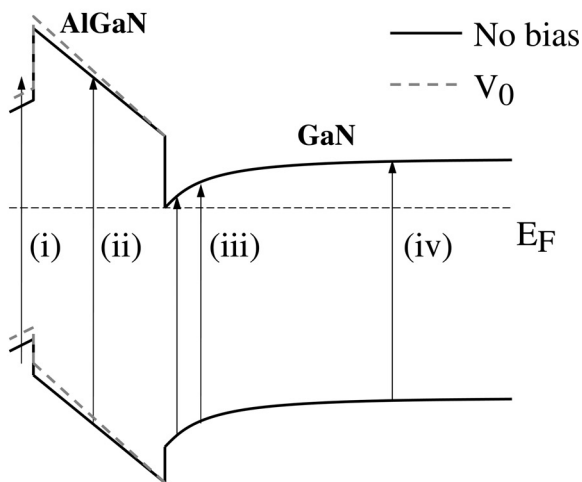
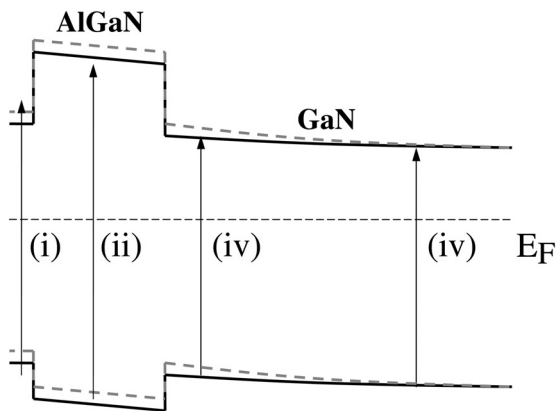
**(a) Polar AlGa<sub>N</sub>/Ga<sub>N</sub> heterostructure****(b) Unpolar AlGa<sub>N</sub>/Ga<sub>N</sub> heterostructure**

FIG. 5. Sketch of band bending and optical transitions in (a) polar and (b) nonpolar AlGa<sub>N</sub>/Ga<sub>N</sub> heterostructures. (i) optical transition in Ga<sub>N</sub> surface quantum well; (ii) band-to-band transition in AlGa<sub>N</sub> layer; (iii) band-to-band transition in Ga<sub>N</sub> buffer layer; (iv) excitonic transition in Ga<sub>N</sub> buffer layer.

phenomenon is present for these heterostructures because no 2DEG is expected at the AlGa<sub>N</sub>/Ga<sub>N</sub> interface). In this case, the intensity of the CER signal is more or less proportional to the absorption volume, which is much larger for the Ga<sub>N</sub> buffer layer than for the AlGa<sub>N</sub> layer, and, therefore, the intensity of the AlGa<sub>N</sub> transition is much weaker.

The lack of polarization effects along the nonpolar direction in III-N means that the surface band bending in nonpolar AlGa<sub>N</sub>/Ga<sub>N</sub> heterostructures results from the Fermi-level pinning on the surface and the carrier concentration inside the structure. The band bending and its modulation for an unpolar heterostructure is plotted schematically in Fig. 5(b). In addition, the possible optical transitions are marked by arrows in this sketch. Very similar Ga<sub>N</sub> excitonic transitions are expected for AlGa<sub>N</sub>/Ga<sub>N</sub> heterostructures and Ga<sub>N</sub> layers within the scheme. Such similarities are clearly visible by naked eye in Fig. 2. For a better comparison, CER spectra in the vicinity of Ga<sub>N</sub> transitions have been fitted by Eq. (3), see Fig. 6. The excitons A and B are fitted by one resonance because the energy separation between these tran-

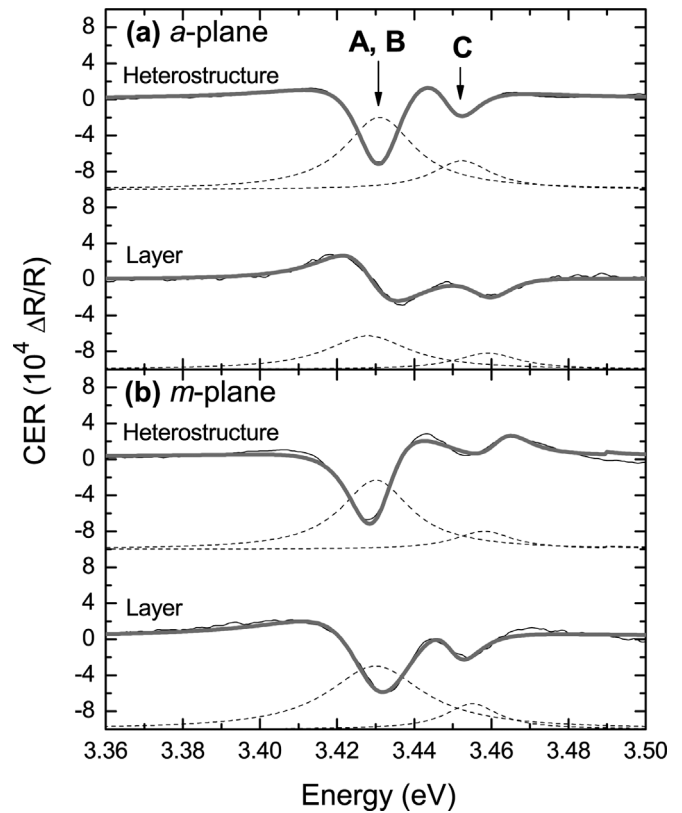


FIG. 6. Room temperature contactless electroreflectance spectra of AlGa<sub>N</sub>/Ga<sub>N</sub> heterostructures and Ga<sub>N</sub> epilayers grown on (a) *a*- and (b) *m*-plane Ga<sub>N</sub> substrate in the vicinity of Ga<sub>N</sub> transition together with the fit (thick gray lines) by Eq. (3) and the moduli of CER resonances (dashed lines).

sitions is much smaller than the broadening of individual exciton lines [5 meV (Ref. 26) vs ~10–15 meV]. Within this analysis, very similar excitonic transitions have been identified as can be seen by comparing the moduli of excitonic resonances. The observed differences between the shape of CER resonances for the AlGa<sub>N</sub>/Ga<sub>N</sub> heterostructure and the Ga<sub>N</sub> layer (that is, various phases of these resonance) appear due to the distance of Ga<sub>N</sub> buffer layer from the surface (that is, the presence of Ga<sub>N</sub> cap and AlGa<sub>N</sub> layer).

For the AlGa<sub>N</sub>/Ga<sub>N</sub> heterostructure grown on the semi-polar Ga<sub>N</sub> substrate, the Ga<sub>N</sub>-related feature is quite broad. However, very similar resonance is also observed for the Ga<sub>N</sub> epilayer with (20.1)-orientation, see Fig. 2(d). It suggests that the quality of the Ga<sub>N</sub> layer grown along this crystallographic orientation is worse than the quality of Ga<sub>N</sub> layers grown along polar and nonpolar directions. On the other hand, a built-in electric field is expected in this heterostructure, but the strong Ga<sub>N</sub> related signal suggests that the 2DEG is rather not present at the AlGa<sub>N</sub>/Ga<sub>N</sub> interface.

It is worth noting that for all AlGa<sub>N</sub>/Ga<sub>N</sub> heterostructures, an optical transition in the Ga<sub>N</sub> cap layer is also expected in CER spectra.<sup>25</sup> Because of quantum confinement, it is located at a higher energy position than that of the Ga<sub>N</sub> energy gap. In our analysis, this transition is neglected because its intensity is much weaker than in the case of Ga<sub>N</sub> excitonic transitions. Moreover, its broadening is quite large because of the width fluctuations of the cap layer. To illustrate this issue, a histogram of optical transitions for an

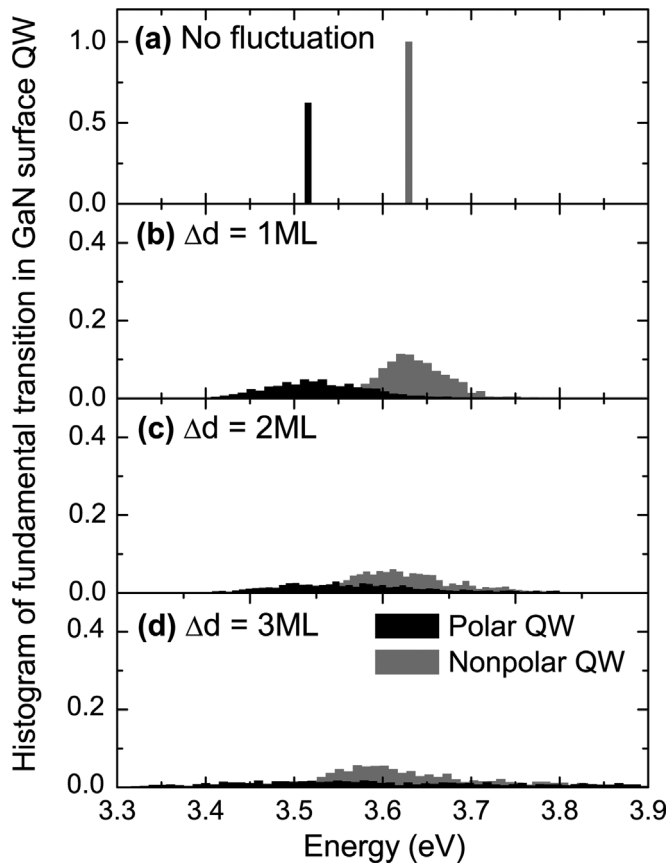


FIG. 7. Histogram of the ground state transition in 2 nm wide GaN surface QW with various inhomogeneities of QW width ( $\Delta d$ ).

inhomogeneous GaN surface quantum well (QW) is calculated and presented in Fig. 7. These calculations were performed according to the model described in Ref. 27 in which the quantum width is treated as a random number with a Gaussian distribution, where the nominal cap width corresponds to the mean value in this distribution and the width fluctuation is the deviation from the main value. Figure 7 clearly shows that the broadening of QW transition increased, and its intensity decreased very significantly when the QW width fluctuation was increased. In our samples, the surface roughness can be even on the level of  $\sim 2$  monolayers (MLs). For such QW inhomogeneities, a very broad and weak CER resonance is expected, which is very consistent with our experimental data, see CER spectrum for the polar AlGaIn/GaN heterostructure in Fig. 2(a).

#### IV. CONCLUSION

In conclusion, CER features typical of FET heterostructures with a strong built-in electric field and 2DEG (that is, AlGaIn-related FKO and the screening of band bending modulation in the GaN buffer layer) are observed only for the AlGaIn/GaN heterostructures grown on the *c*-plane substrate. When the same AlGaIn/GaN heterostructures are grown on nonpolar or semipolar GaN substrates, any CER features that could be related to a strong built-in electric field in the AlGaIn layer or the 2DEG presence at the interface are not visible in CER spectra. It means that modula-

tion doping is necessary for nonpolar and semipolar AlGaIn/GaN FET heterostructures and the total depletion of the 2DEG will be possible in such heterostructures.

#### ACKNOWLEDGMENTS

This work was supported by Polish Ministry of Science and Higher Education under Grants No. 6 ZR6 2009C/07280 (“Opracowanie i wdrożenie technologii produkcji niepolarnych podłoży GaN”) and N515054635, National Centre for Research and Development (Grant No. LIDER/14/192/L-1/09/NCBIR/2010), and the Ministry of Regional Development (Grant No. POIG.01.01.02-00-015/09-00). In addition, R.K. acknowledges the support from the Foundation for Polish Science (Grant HOMMING).

<sup>1</sup>F. Bernardini and V. Fiorentini, *Phys. Rev. B* **64**, 085207 (2001).

<sup>2</sup>O. Ambacher, J. A. Majewski, C. Miskys, A. Link, M. Hermann, M. Eickhoff, M. Stutzmann, F. Bernardini, V. Fiorentini, V. Tilak, B. Schaff, and L. F. Eastman, *J. Phys.: Condens. Matter*, **14**, 3399 (2002).

<sup>3</sup>See, for example, the Proceeding of 8th International Conference on Nitride Semiconductors in Korea published in *Phys. Status Solidi* **7**, (2010).

<sup>4</sup>M. Kuroda, H. Ishida, T. Ueda, and T. Tanaka, *J. Appl. Phys.* **102**, 093703 (2007).

<sup>5</sup>S. L. Selvaraj and T. Egawa, *Jpn. J. Appl. Phys.* **47**, 3332 (2008).

<sup>6</sup>S. Arulkumar, S. Lawrence Selvaraj, T. Egawa, and G. I. Ng, *Appl. Phys. Lett.* **92**, 092116 (2008).

<sup>7</sup>C. Y. Chang, Y.-L. Wang, B. P. Gila, A. P. Gerger, S. J. Pearton, C. F. Lo, F. Ren, Q. Sun, Y. Zhang, and J. Han, *Appl. Phys. Lett.* **95**, 082110 (2009).

<sup>8</sup>R. Dwilinski, R. Doradzinski, J. Garczynski, L. Sierzputowski, R. Kucharski, M. Zajac, M. Rudzinski, R. Kudrawiec, J. Serafiniczuk, and W. Strupinski, *J. Cryst. Growth* **312**, 2499 (2010).

<sup>9</sup>R. Kucharski, M. Rudzinski, M. Zajac, R. Doradzinski, J. Garczynski, L. Sierzputowski, R. Kudrawiec, J. Serafiniczuk, W. Strupinski, and R. Dwilinski, *Appl. Phys. Lett.* **95**, 131119 (2009).

<sup>10</sup>R. Kudrawiec, M. Rudzinski, R. Kucharski, M. Zajac, R. Doradzinski, L.P. Sierzputowski, J. Rarczynski, J. Serafiniczuk, W. Strupinski, J. Misiewicz, and R. Dwilinski, *Phys. Status Solidi C* **7**, 2359 (2010).

<sup>11</sup>R. Kucharski, M. Zajac, R. Doradzinski, J. Graczynski, L. Sierzputowski, R. Kudrawiec, J. Serafiniczuk, J. Misiewicz, and R. Dwilinski, *Appl. Phys. Express* **3**, 101001 (2010).

<sup>12</sup>M. Munoz, S. Guo, X. Zhou, M. C. Tamargo, Y. S. Huang, C. Trallero-Giner, and A. H. Rodriguez, *Appl. Phys. Lett.* **83**, 4399 (2003); M. Motyka, R. Kudrawiec, G. Sek, J. Misiewicz, I. L. Krestnikov, S. Mikhlin, and A. Kovsh, *Semicond. Sci. Technol.* **21**, 1402 (2006); M. Motyka, R. Kudrawiec, G. Sek, J. Misiewicz, D. Bisping, B. Marquardt, A. Forchel, and M. Fischer, *Appl. Phys. Lett.* **90**, 221112 (2007).

<sup>13</sup>R. Kudrawiec, M. Gladysiewicz, J. Misiewicz, F. Ishikawa, and K. H. Ploog, *Appl. Phys. Lett.* **90**, 041916 (2007); R. Kudrawiec, M. Gladysiewicz, J. Misiewicz, H. B. Yuen, S. R. Bank, M. A. Wistey, H. P. Bae, and J. S. Harris, Jr., *Phys. Rev. B* **73**, 245413 (2006).

<sup>14</sup>Y. S. Huang, W. D. Sun, F. H. Pollak, J. L. Freeouf, I. D. Calder, and R. E. Mallard, *Appl. Phys. Lett.* **73**, 214 (1998).

<sup>15</sup>D. Y. Lin, Y. S. Huang, T. S. Shou, K. K. Tiong, and F. H. Pollak, *J. Appl. Phys.* **90**, 6421 (2001).

<sup>16</sup>R. Kudrawiec, M. Syperek, M. Motyka, J. Misiewicz, R. Paszkiewicz, B. Paszkiewicz, and M. Tlaczala, *J. Appl. Phys.* **100**, 013501 (2006).

<sup>17</sup>R. Kudrawiec, B. Paszkiewicz, M. Motyka, J. Misiewicz, J. Derluyn, A. Lorenz, K. Cheng, J. Das, and M. Germain, *J. Appl. Phys.* **104**, 096108 (2008).

<sup>18</sup>D. Y. Lin, J. D. Wu, J. Y. Zheng, and C. F. Lin, *Physica E* **40**, 1763 (2008).

<sup>19</sup>R. Kudrawiec, *Phys. Status Solidi B* **247**, 1616 (2010).

<sup>20</sup>D. E. Aspnes and A. A. Studna, *Phys. Rev. B* **7**, 4605 (1973); H. Shen and M. Dutta, *J. Appl. Phys.* **78**, 2151 (1995).

<sup>21</sup>R. Kudrawiec, M. Motyka, J. Misiewicz, B. Paszkiewicz, R. Paszkiewicz, and M. Tlaczala, *Microelectron. J* **40**, 370 (2008).

- <sup>22</sup>M. Motyka, R. Kudrawiec, M. Syperek, J. Misiewicz, M. Rudzinski, P. Hageman, and P. K. Larsen, *Thin Solid Films* **515**, 4662 (2007).
- <sup>23</sup>I. Vurgaftman and J. R. Meyer, *J. Appl. Phys.* **94**, 3675 (2003).
- <sup>24</sup>D. E. Aspnes, *Surf. Sci.* **37**, 418 (1973).
- <sup>25</sup>M. Motyka, M. Syperek, R. Kudrawiec, J. Misiewicz, M. Rudzinski, P. R. Hageman, and P. K. Larsen, *Appl. Phys. Lett.* **89**, 231912 (2006); R. Kudrawiec, M. Gladysiewicz, J. Misiewicz, R. Paszkiewicz, B. Paszkiewicz, and M. Tlaczala, *AIP Conf. Proc* **1199**, 25 (2009).
- <sup>26</sup>R. Kudrawiec, M. Rudzinski, J. Serafinczuk, and M. Zajac, *J. Appl. Phys.* **105**, 093541 (2009).
- <sup>27</sup>M. Gladysiewicz and R. Kudrawiec, *J. Phys.: Cond. Mater.* **22**, 485801 (2010).